CLOUD-CHAMBER OBSERVATIONS OF COSMIC RAYS AT HIGH ALTITUDE

Thesis by

Eugene Woodville Cowan

In Partial Fulfillment of the Requirements

For the Degree of

Doctor of Philosophy

California Institute of Technology

Pasadena, California

1948

Acknowledgements

Credit and thanks are due the U. S. Navy and Army Air Force personnel at Inyokern, California, and in particular to Commander E. Bollay of the Office of Naval Research, for making possible the B-29 airplane flights. This work was supported in part by U. S. Navy Contract ONR-Physics-13.

I am also indebted to Dr. Carl D. Anderson, my thesis supervisor, and Dr. Paul E. Lloyd for their interest and advice in connection with problems that have arisen.

Abstract

Measurements of the distribution of zenith angles of large air showers made with a large cloud chamber at an altitude of 10,200 meters show the distribution to be much narrower about the vertical than that predicted by present shower theory. Although several experimental errors are present, the corrections are in such a direction as to augment the disagreement.

Evidence in the form of an elastic collision with an electron has been found for the existence in cosmic rays at high altitude of a low-mass mesotron. The mass as calculated from the angles of the elastic collision is approximately 13 times the mass of an electron. Since two such collisions occur on the same track, the probability of their being chance coincidences of nuclear deflections and knock-on electrons is small - - of the order of one in ten million.

Table of Contents

I

Cloud Chamber

A cylindrical cloud chamber of diameter 87 cm and depth 15 cm was used in making the observations discussed in this report. The chamber was mounted in the after pressurized cabin of a B-29 airplane with the axis of the cylinder horizontal. Twenty-six flights in which approximately 3500 photographs were taken were made at altitudes ranging up to 13,500 meters above sea level. A magnetic field was not used. Photographic views of the equipment are shown in Figs. 1 and 2. The cloud chamber itself was designed and constructed by C. D. Anderson and S. H. Neddermeyer in 1937, and the auxiliary control and photographic apparatus was then added especially for this series of flights.

1.1. Expansion. The cross-sectional drawing in Fig. 3 indicates the method used to obtain an axial expansion. A circular diaphragm connected to the chamber by a ringlike rubber membrane is supported by rollers resting on the lower part of the chamber walls. Compressed air admitted to the cavity behind

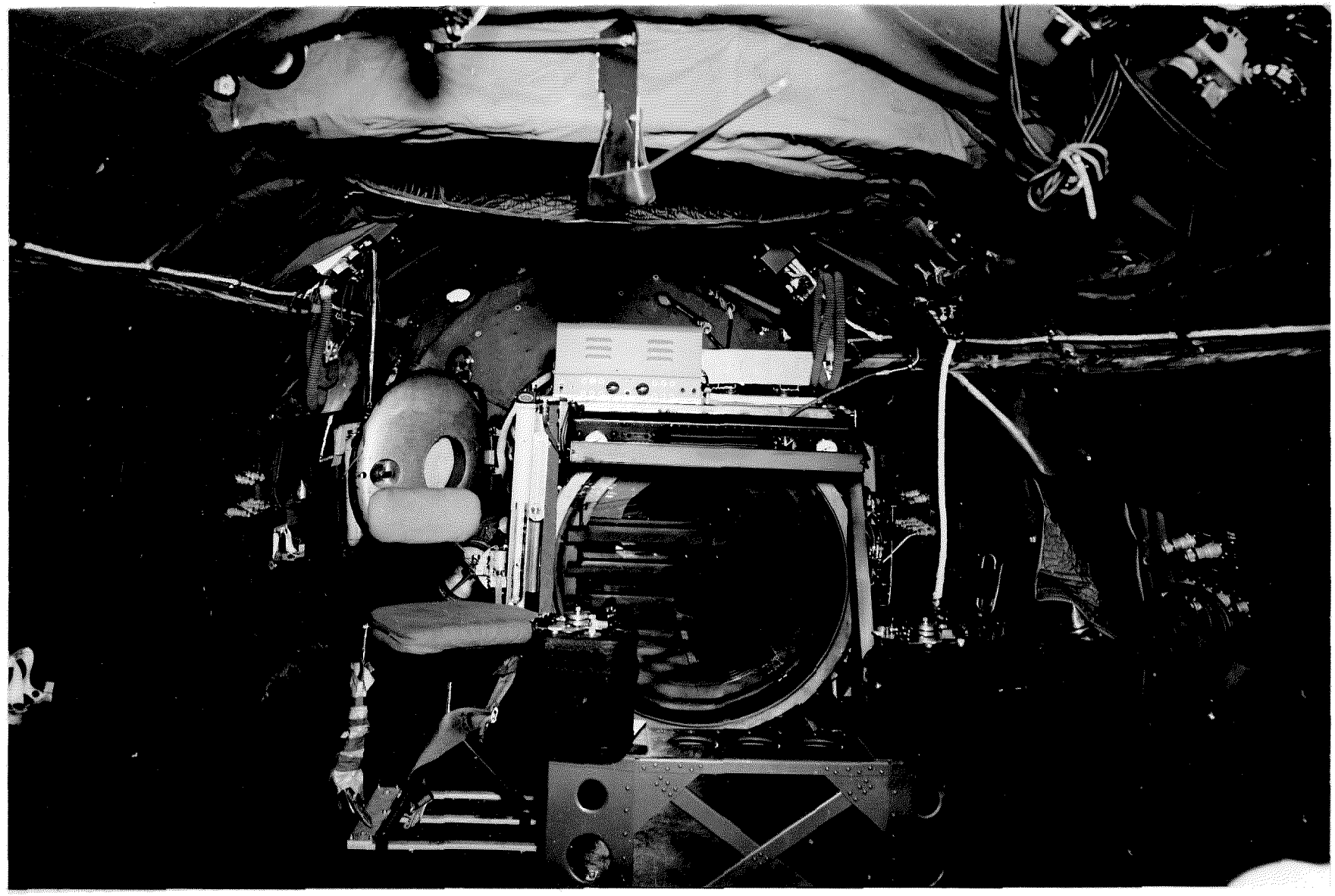

Fig. 1. Front view of cloud chamber, showing cameras.

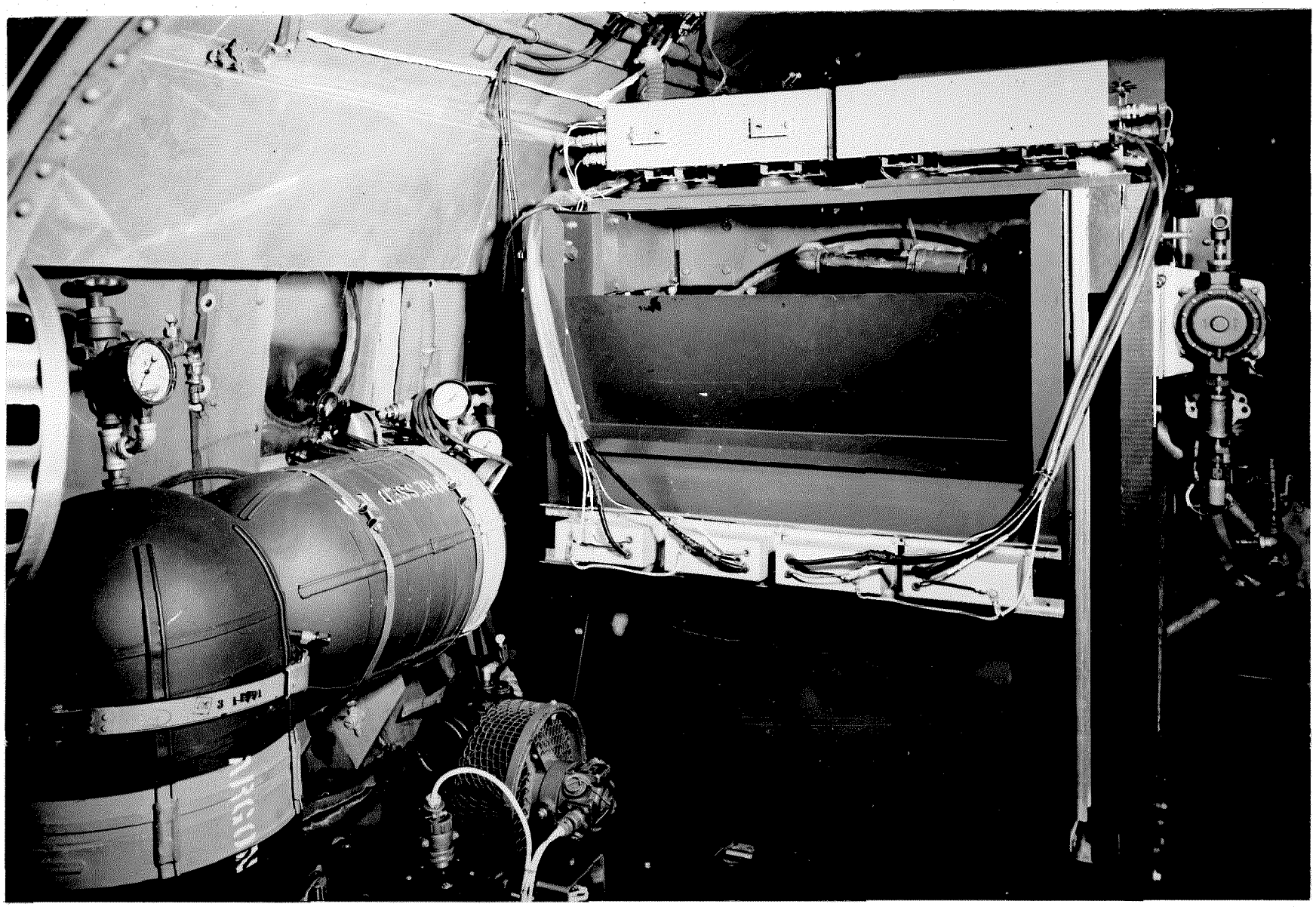

Fig. 2. Rear view of cloud chamber, showing lighting system.

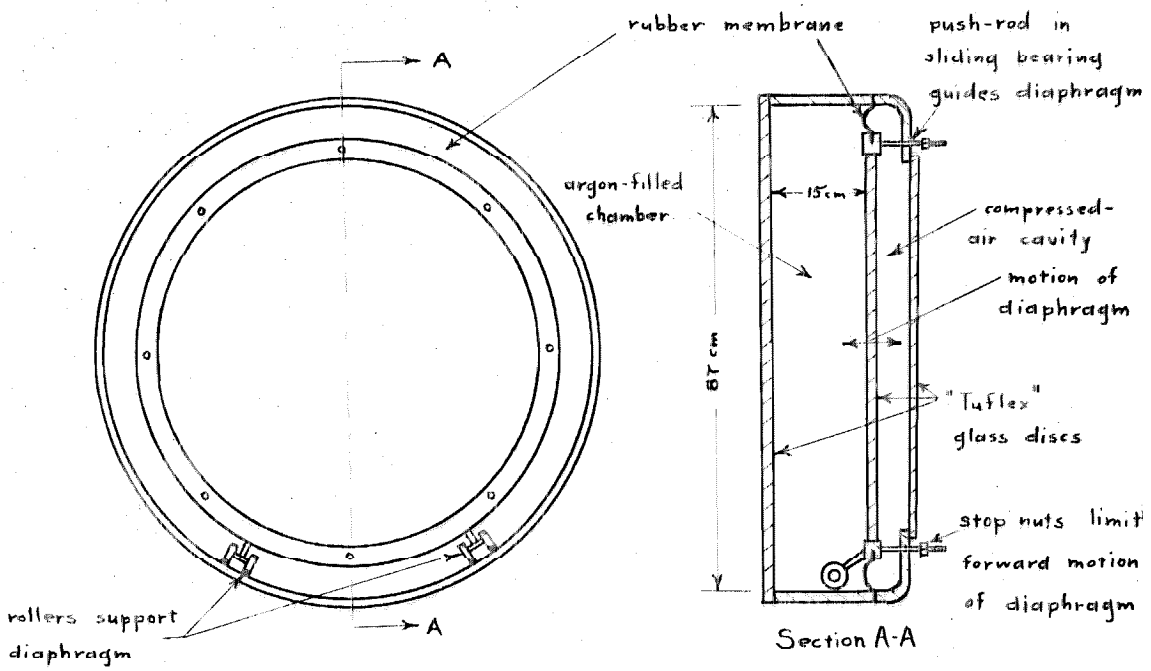

Fig. 3. Method of Obtaining Expansion.

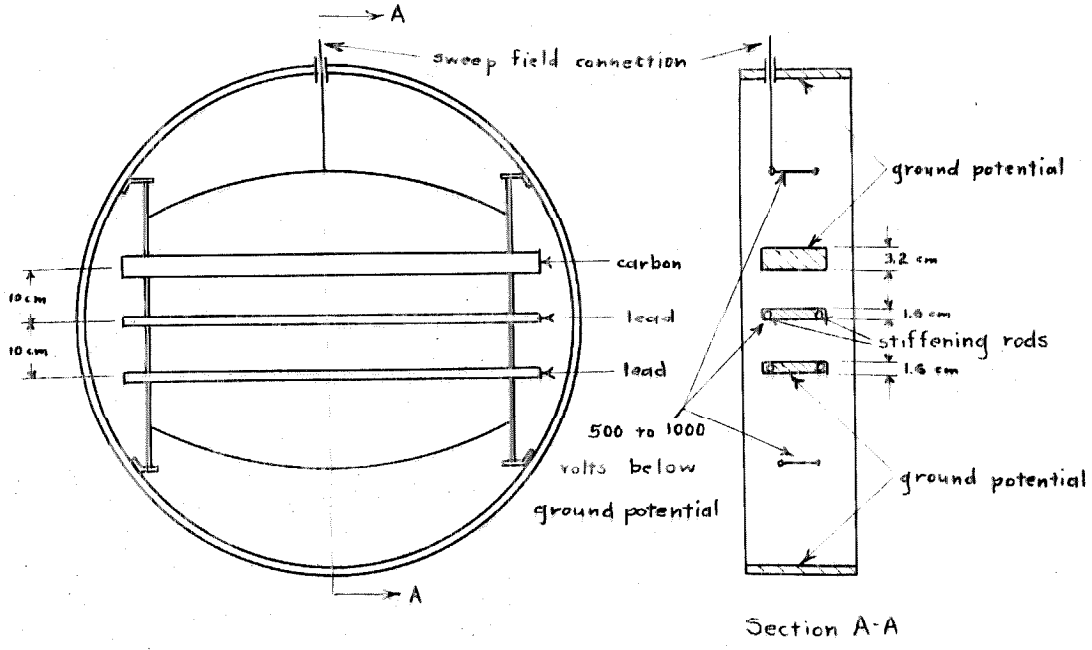

Fig. 4. Arrangement of Plates in Chamber.

the diaphragm (on the side opposite to that of the cloud chamber) moves the diaphragm forward and compresses the gas in the chamber, which is initially 10 or 20 cm Hg pressure above the surrounding cabin pressure. Expansion is accomplished by suddenly releasing this compressed air into the cabin through a large valve.

Eight equally-spaced push-rods are connected to the edge of the diaphragm and pass through sliding bearings in the rim of the cavity behind the chamber to aid in guiding the diaphragm. Alternate push-rods are supplied with adjustable nuts that limit the forward motion of the diaphragm and thus control the expansion ratio. Springs on the other push-rods are adjustable so that the diaphragm will remain perpendicular to the axis of the chamber during the expansion.

1.2. Chamber Interior. Figure 4 shows the manner in which the three plates are arranged inside the chamber. The dimensions of the plates in order from top to bottom are as follows: (1) carbon, 77.3 cm by 11.3 cm by 3.2 cm, (2) and (3) lead, 77.3 cm by 11.3 cm by 1.6 cm. Additional stiffening for the lead plates was obtained by casting the plates with two pieces of

steel tubing running the length of the plates near the edges in the position indicated in Fig. 4. A row of holes drilled in the tubing insure that lead filled the tubes during the casting process. From the viewpoint of mass per square centimeter, the plates may therefore be considered with only a small approximation to be of solid lead.

Four wires, supported above and below the set of plates, and the cen ter one of the three plates, may be given a potential of from 500 to 1000 volts negative with respect to the outer two plates and the chamber walls to provide a sweep field for the chamber (see Fig. 4). An electric field of the order of 50 to 100 volts per centimeter is thus maintained in the chamber until the moment of expansion. As the diaphragm moves to expand the chamber, a mechanism connected to the topmost diaphragm push-rod short-circuits the sweep-field circuit and reduces the sweep field to a small value. Simultaneously the same mechanism uncovers a small hole and drops a b-b shot, which, after dropping down behind the chamber, is photographed in the midst of its fall by the flash of light illuminating the chamber. This is used to give a measure of the sensitive time of the chamber, as discussed in section 2.2.

Argon gas saturated with ethyl-alcohol vapor has been used to fill the chamber for all of the photographs discussed in this report. In order to insure that the gas near the top of the chamber is saturated with alcohol vapor, alcohol is pumped from a small pool in the bottom of the chamber through a filter and check valve up to two small pipes entering the top of the chamber. From these pipes the alcohol squirts onto the rubber membrane and runs down again to the pool at the bottom of the chamber, providing a surface of alcohol of considerable extent at which evaporation can take place.

1.3. Cameras and Illumination. Two Type K-25 aerial cameras were modified by adding an 0.75-diopter lens immediately in front of the camera lens, which is normally focused for taking pictures at large distances. The cameras are placed as shown in Fig. 5 to take simultaneous pictures from different angles to give a stereoscopic view of the chamber. Each camera takes 50 pictures, 13.9 cm by 11.4 cm, on a 6-meter roll of triple-X (exposure index 200) panchromatic film. Most of the pictures have been taken with a lens aperture of f-16.

Illumination is provided by 4 krypton-filled flash bulbs, each connected to a 23-μf condenser charged to a potential of

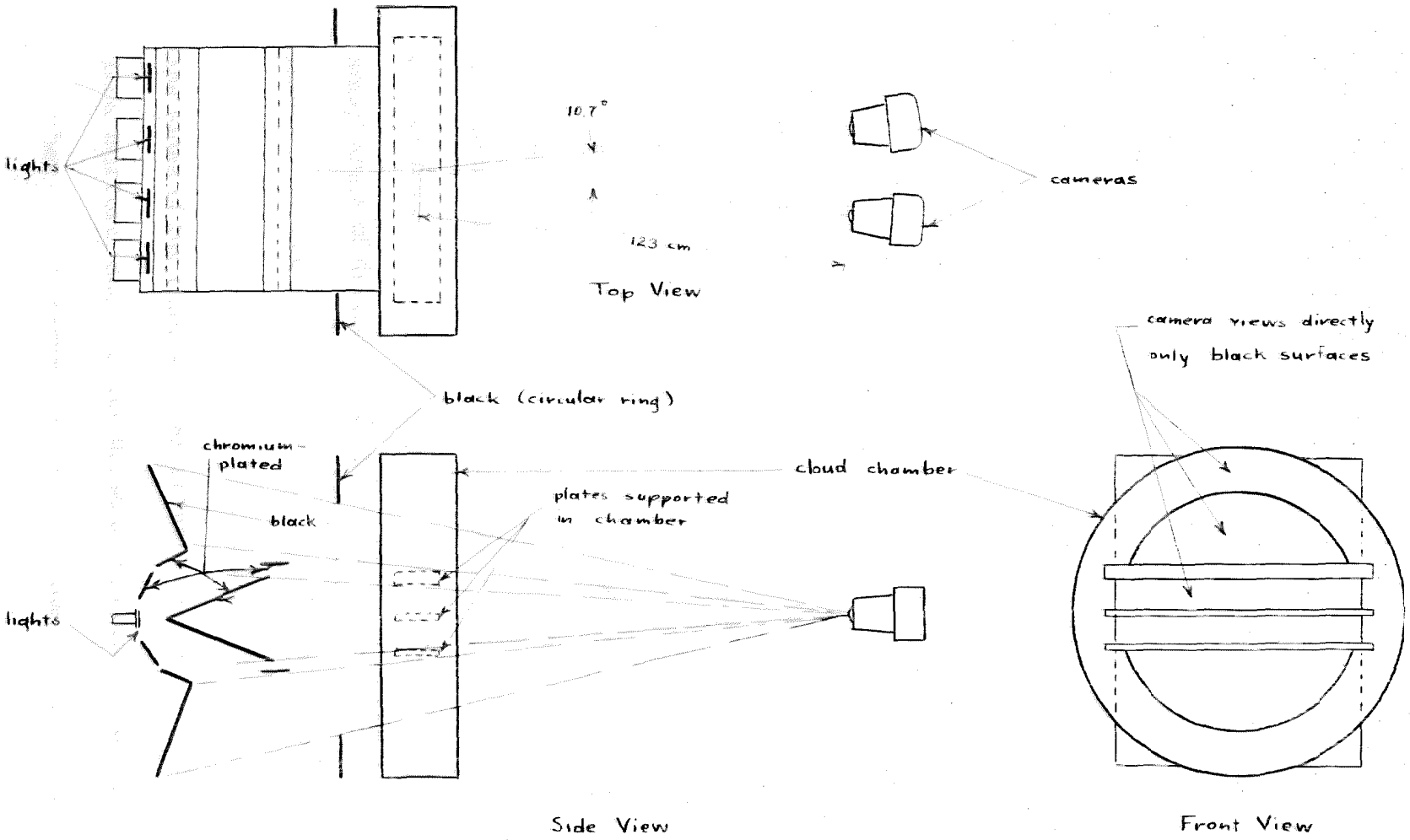

Fig. 5. Cameras and Illumination.

2000 volts. These flash bulbs and their power supplies are part of a Model S-1169 Army Signal Corps light identification unit. Since this unit was designed to operate on the standard 28-volt d-c aircraft supply, it could be used with only minor modifications. Four of the Model X-400 flash-bulb units arranged in a straight line approximate the desired line source and are rugged and simple to mount.

The front plate of the chamber, the diaphragm, and the back plate of the air-filled cavity behind the chamber are all of "Tuflex" glass so that the chamber is essentially three transparent circular discs arranged to form a cylinder, with the center disc the movable diaphragm. This allows the chamber to be illuminated from the rear (side opposite from that of the cameras) as shown in Fig. 5. Because the spherical droplets in the chamber scatter many times more light in a given solid angle through a small angle of deviation than through a large angle, such rear illumination requires only a small fraction of the energy for lighting demanded by right-angle illumination with the light sources at the sides of the chamber. An arrangement of chromium-plated iron mirrors, shown in the drawing, distributes the light in the chamber so that tracks in all parts of the chamber scatter

approximately equal amounts of light into the cameras. This allows a compact arrangement with the lights close to the chamber. Direct rays of light and rays scattered through only a very small angle are prevented from entering the cameras by arranging the source and mirrors so they are hidden behind the carbon and lead plates mounted in the chamber, in the manner indicated in the diagram.

1.4. Control. Regulation of the air pressure which controls the position of the diaphragm is accomplished by means of high and low pressure reducer valves and electrically operated shut-off valves. The air is dried to prevent the appearance of a cloud of water droplets behind the diaphragm on expansion and is warmed to prevent cooling of the diaphragm and the resultant condensation of alcohol on the chamber side of the glass.

Operation of the chamber is controlled electrically by means of conventional circuits. Pictures have been taken both with the chamber expanded at predetermined intervals and with counter control. A typical cycle of operation with the former type of control, which is entirely automatic, is as follows on the next page.

Time in Seconds	Event
0	fast-timing motor starts
2	fast expansion
2.1	cameras start, visual lights go out, and mechanical counter operates
2.2	both shutters open and lights flash
2.5	shutters close, visual lights come on, and cameras stop
5	fast timing motor stops
5	compressed-air valve opens and chamber is recompressed
20	slow expansion
37	chamber recompresses
60	alcohol pump starts
64	alcohol pump stops
80	fast timing motor starts again

If the slow expansion is omitted, and this is possible after the chamber has been expanded a few times, the total time required for one cycle is approximately one minute.

Control of the chamber with counters was accomplished through the cooperation of Dr. M. Schein and Mr. H. L. Kraybill, of the University of Chicago, who had installed counters and

coincidence circuits in the B-29 for measuring the frequency of large air showers. Figure 7 shows the arrangement of the three counters placed 1.37 meters apart in a horizontal plane above the chamber. Each counter has a cylindrical sensitive volume 33 cm long and 2.5 cm in diameter. The triple coincidence necessary to trip the chamber is obtained about once every $2\frac{1}{2}$ minutes at an altitude of 10,200 meters.

An auxiliary circuit, consisting of a charged condenser connected to the coil of the trip through a cold-cathode trigger tube, enables the pulse from the coincidence circuits to operate the chamber trip, which in turn by means of an electric-contact arm starts the cameras. The switch preventing operation of the trip during the recovery period (about 30 seconds) and the switches controlling the alcohol pump and slow expansion are operated manually with the timing motors turned off for counter-controlled operation.

The motion of the diaphragm is slower and therefore the tracks with counter-tripped operation more diffuse than with a small chamber, since the mass of a diaphragm increases with the cube of the linear dimensions while the area and moving force increase with the square. With correct adjustment of the light

delay, however, fairly sharp tracks can be obtained with counter-tripped operation.

1.5. Operation. The following comments about the operation of the chamber may prove useful to any future user. Argon is introduced slowly into the chamber through the alcohol drain hole at the bottom, displacing the lighter air out through the alcohol pipes at the top. Enough alcohol is poured in to form a pool in the bottom of the chamber. It is important to use sufficient alcohol so that no gas is sucked into the alcohol piping system when the pump is operating, since when this gas is later expelled into the chamber, it forms clouds of droplets upon expansion. The alcohol pump must not be operated unless there is sufficient pressure behind the diaphragm to bow the rubber forward, or alcohol may be splattered on the glass. Although the manometer lines are left open to the chamber during expansion, no trouble with "spurts" or local overexpansion has been experienced except a cloud of droplets from a slightly porous region in the lower lead plate, which was remedied by a second coat of paint.

A value of sweep voltage of from 500 to 1000 volts is satisfactory, higher voltages producing corona, and lower voltages giving a heavy background fog with the larger ionization of the gas in the chamber at high altitude. A small amount of corona

(visible in some of the photographs as a streamer of droplets from a fine piece of lint adhering to one of the lower sweep-field wires) does not seem to seriously contaminate the chamber.

After the chamber has been filled in the expanded position to a pressure of 10 to 20 cm Hg above the outside pressure, the air pressure behind the diaphragm is increased until it exceeds the chamber pressure by 1 to 5 cm Hg, the chamber then being in the compressed position. Since the rubber part of the diaphragm is not perfectly stiff, changing the differential pressure across the diaphragm changes slightly the chamber volume even when the diaphragm is against the stops, thus providing a fine adjustment of the expansion ratio in addition to the rather coarse mechanical adjustment of the stops.

Adjustment of the springs that control the angle of the diaphragm during its movement is best accomplished by watching the movement of the reflected image of a small light in the glass plates as the chamber expands.

Although several slow expansions are necessary when first placing the chamber in operation, further slow expansions are not necessary, even at high altitude, allowing the time of a cycle of operation to be shortened by this amount. It has been observed that the chamber is sensitive to the heavily ionizing part-

icles from nuclear disintegrations at high altitudes for a relatively long time during a slow expansion, especially if the expansion is very slow and somewhat larger than normal. This suggests that absolute "star" intensity at high altitudes might be measured by photographing the chamber during such operation with a movie camera.

II

Interpretation of Data

2.1. Instruments Recorded on Film. An instrument panel mounted above the chamber contains four instruments and three lettered cards, which appear in each photograph with the chamber. See, for instance, Fig. 6 on the next page. From left to right the instruments are as follows: (1) chamber pressure gauge, reading in pounds per square inch above cabin pressure (the pressure reading existing just before the expansion is obtained in the photograph because of a porous plug in the line to the gauge), (2) mechanical counter, which advances one digit before each picture, allowing easy correlation later of the two stereoscopic views, (3) altimeter, reading in hundreds, thousands, and tens of thousands of feet for the three hands in the order of reducing size, (4) cabin pressure gauge, reading in pounds per square inch below one atmosphere. The lettered cards show the the flight number, date, and destination, if the flight is other than a local one.

For flights 1 through 9, the pressure in the chamber when expanded was approximately 10 cm Hg above cabin pressure

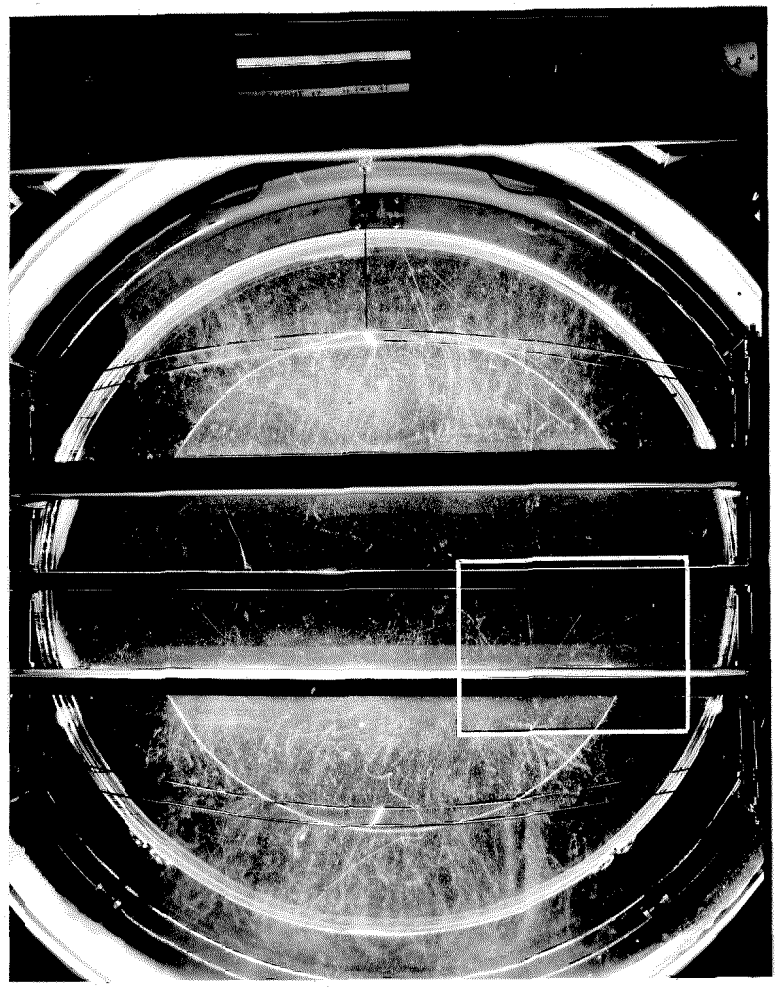

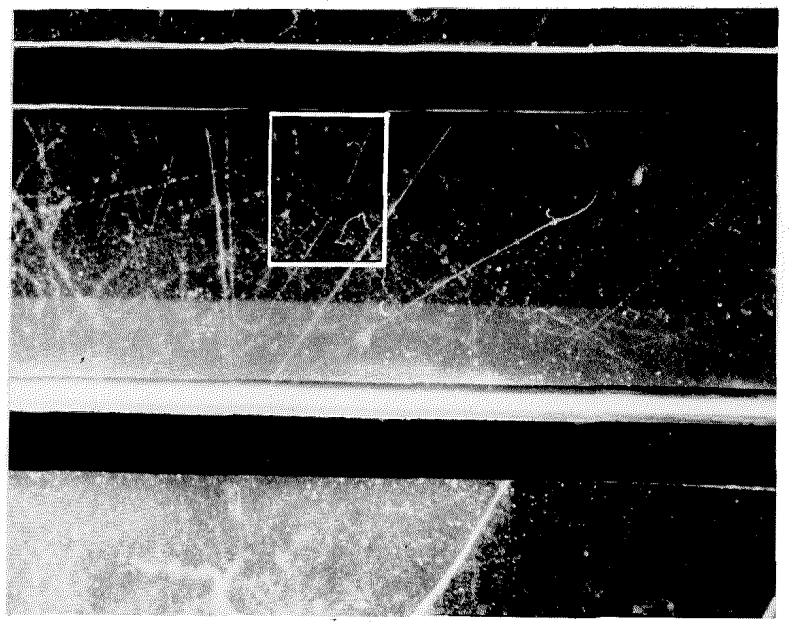

Fig. 6. Typical chamber photograph (long light delay) at 12,100 meters altitude. Enlargements show detail in right center of picture.

and when compressed 15 cm Hg above cabin pressure, while for flights 10 through 20, these figures were doubled. At altitudes between 5,000 and 10,000 meters, the pressure inside the pressurized cabin was approximately 20 cm Hg below one atmosphere. Therefore, for most of the photographs the absolute pressure in the chamber when compressed was slightly above one atmosphere and when expanded, slightly below one atmosphere. Whether a track has been caused by a particle passing through before or after the expansion can be determined in many cases by the effect of the sweep field, which is turned off during the expansion.

The temperature in the cabin ranged from 0 to 20° C, tending toward the latter figure on the flights in which most of the photographs were taken. At 20° C the vapor pressure of ethyl alcohol is 8 cm Hg so that about 90 per cent of the atoms in the chamber gas were argon, 7 per cent hydrogen, 2 per cent carbon, and 1 per cent oxygen.

The altimeter was set to read altitude above sea level for the first 12 flights but changed to read pressure altitude for subsequent flights.

2.2. Sensitive Time. To obtain from the count of any particular type of event appearing in the photographs the absolute

frequency of occurrence of that event requires a knowledge of the time during which the chamber was sensitive to cosmic-ray particles preceding the photograph. Although information regarding the sensitive time was not needed for the analysis of the photographs presented in this thesis, the following information concerning three methods experimented with to obtain the sensitive time may be useful in any future analysis of the data.

The first method consisted of generating pulses of ions in the chamber at regular time intervals just before the photograph was taken by applying pulses of voltage to a needle protruding into the chamber. Corona from the sharp point produced a small cloud of ions for each voltage pulse, giving droplets about ions generated at a known time for comparison in size with droplets formed about ions produced by cosmic rays. Voltage pulses of 1200 volts at intervals of approximately 30 milliseconds were tried, and a separate blob of droplets for each pulse could be clearly distinguished on the photographs. However, in view of the unknown accuracy of this method, a second and probably more accurate method was devised.

A separate set of lights was supplied for each of the two cameras. One set of lights was arranged to be flashed at a time

after the expansion sufficiently long for droplets to grow large enough to be photographed and the other set to be flashed about 0.1 sec later. The camera shutters were synchronized in such a manner that each camera was affected by only one flash of light. Any droplets appearing in one photograph and not in the other must then have grown to a size sufficiently large to be photographed in the interval between the flashes. Consequently a known length of time is established for a certain set of tracks to have passed through the chamber.

Although the control circuits are wired so that at present the above type of operation may be selected by throwing a switch mounted on one camera, this type of operation was found to be impractical at high altitude because the large number of tracks in each photograph make essential the use of stereoscopic views. Since only those tracks that are in the chamber preceding the first flash appear in both photographs and can be viewed stereoscopically, still a third method was used to determine the sensitive time for most of the pictures.

As described in section 1.2, a b-b shot is dropped simultaneously with the short-circuiting of the sweep-field voltage by a mechanism actuated by the motion of the diaphragm during

the expansion. After dropping down behind the chamber, the b-b shot is photographed in the midst of its fall. See, for instance, Fig. 6, in which the b-b shot appears just below the lower lead plate near the middle of the chamber. From the distance that the shot has fallen, the length of time between the removal of the sweep-field voltage and the flash of light making the photograph may be calculated.

All tracks whose ions have not been separated by the sweep field must then have passed through the chamber in this interval minus the time for droplets to grow large enough to be photographed, this then being the sensitive time for unseparated tracks, provided the chamber was still sensitive at the instant the photograph was taken. The most serious limitations on the accuracy of this method appear to be: (1) it is impossible to remove the sweep field entirely, especially in some regions of the chamber, because of residual charges left on the glass walls, and (2) regions of gas in the chamber near the walls and lead plates may be warmed sufficiently rapidly after the cooling caused by the expansion so that droplets are not formed about ions produced in the latter part of the period just before the light flash. A check on the influence of both of these factors can be made by taking

motion pictures of the chamber during and immediately after an expansion.

2.3. Information from Tracks. Tracks appearing in the photographs reveal considerable information regarding the particles making the tracks besides direction and number. The density of ionization left along the track, and therefore the density of droplets, is a function of the velocity and charge of the passing particle but not of the mass, since the mass does not influence the forces involved nor the length of time for which they act. The density of ionization is a minimum for a velocity about 97 per cent of that of light and increases approximately as the reciprocal of the square of the velocity for lower velocities.

Accuracy of measurement of density of ionization is severely limited for "fresh" tracks in which the ions have not had an opportunity to spread and the droplets are therefore very close together. In such cases the apparent density of a track depends more on the illumination than on the actual density of ionization, and often the only information obtainable is that the velocity is less than that for minimum ionization. This can usually be ascertained by whether a track appears smooth and continuous rather than consisting of discrete blobs of ions, regardless of the

apparent "heaviness" of the track. For more diffuse tracks, an estimate of the number of droplets is possible, and a more accurate measure of ionization and velocity is obtainable. In estimating ionization, and in particular the rate of change of ionization, with distance along a track, the rapid decrease of illumination near the walls of the chamber and the plates must be considered, as must the angle at which the track is viewed.

The mean scattering of a track, that is the average of the angular deflection from a straight line for given increments of track length, is a function of the velocity, charge, and mass of the moving particle. For multiple scattering, where the resultant deflection is the result of many small deviations, the statistical average of the resultant is approximately inversely proportional to the kinetic energy if the velocity is small compared to that of light.

Distortion of the tracks because of motion of the gas in mass in the chamber introduces most of the error in the measurement of scattering, provided that the direction of the track in the chamber does not make stereoscopic viewing difficult. This distortion increases with the length of time that the track has been in the chamber and is largest near the plates and sweep-

field wires, where turbulent air motion is caused by the expansion. If a particle passes through the chamber before the sweep field is turned off, the track may also be badly distorted by the influence of the sweep field on the ions. Particularly if the scattering is small, it is very difficult to distinguish between distortion and scattering.

Theoretically, given both the scattering and ionization, and with the assumption of unit electronic charge, the mass of the particle leaving the track may be calculated. However, since accurate scattering measurements require that the track be fresh, while accurate ionization measurements require that the track be old, conditions under which a reasonable estimate of both can simultaneously be made are rare.

If the particle stops in the gas of the chamber, then either the scattering or the ionization coupled with the residual range gives an estimate of the mass of the particle. The range of a particle is directly proportional to its mass and depends also upon the charge and velocity. An immediate clue as to the identity of a particle is furnished by the appearance of the track near the end of its range. The enlargements of a small region of the photograph in Fig. 6 show a typical electron track ending in the

gas, and several straight proton tracks (ionizing many times the minimum value) from a nuclear disintegration in the lower lead plate. This photograph gives some idea of the large number and variety of tracks obtained upon each expansion of the chamber at high altitude.

In some of the later flights the length of time the light was delayed after the expansion was considerably reduced to decrease the number of tracks and resultant confusion in each photograph. When the pictures are viewed stereoscopically, the effect of separating the tracks in a third dimension makes their interpretation a great deal easier and clearer. Views from both cameras are furnished in one of the enlargements in Fig. 6, and these may be viewed stereoscopically by holding them 3 or 4 feet from the eye and looking past them at a distant object until the left picture as seen by the left eye merges with the right picture viewed by the right eye. The successive enlargements show the excellent resolution of the photographs, some of which was lost in the printing process.

Passage of a track through one or more of the plates in the chamber also furnishes information about the nature of the particle. Since each of the lead plates is approximately three

radiation units thick, it is very unlikely that any particle passing through one of the plates without multiplying and producing more than one track is an electron. Futhermore if a particle is ionizing more than the minimum value mentioned above and then passes completely through a lead plate, it is a proton rather than a mesotron or lighter particle, since with such a velocity, particles of mass much less than a proton do not have sufficient energy to penetrate one of the lead plates.

Additional information about particles is furnished by elastic collisions as discussed in a later section.

III

Experimental Results and Conclusions

3.1. Large Air Showers. The coincidence-counter control described in section 1.4 was used to trip the chamber for approximately 350 pictures for the purpose of obtaining the statistical distribution of the angle from the zenith of large air showers. It was also hoped that a qualitative idea of the spatial distribution of the shower particles and possibly evidence for a penetrating component might be obtained.

Coincident pulses from three counters, which were arranged above the chamber in a horizontal plane in the manner shown in Fig. 7, were required to trip the chamber. Of the photographs so obtained, 228 taken at an altitude of 10,200 meters and 44 at 12,100 meters were selected solely on the basis of the apparently correct operation of the chamber and without regard to the number of tracks appearing on the photographs. Since the majority of these photographs showed only a few tracks, often not parallel to one another, it was necessary to establish a criterion whereby photographs could be selected for measurement that would yield a unique direction for the shower. Obviously the criterion used affects the statistical angular distribution obtained

Fig. 7

ANGULAR DISTRIBUTION OF LARGE AIR SHOWERS

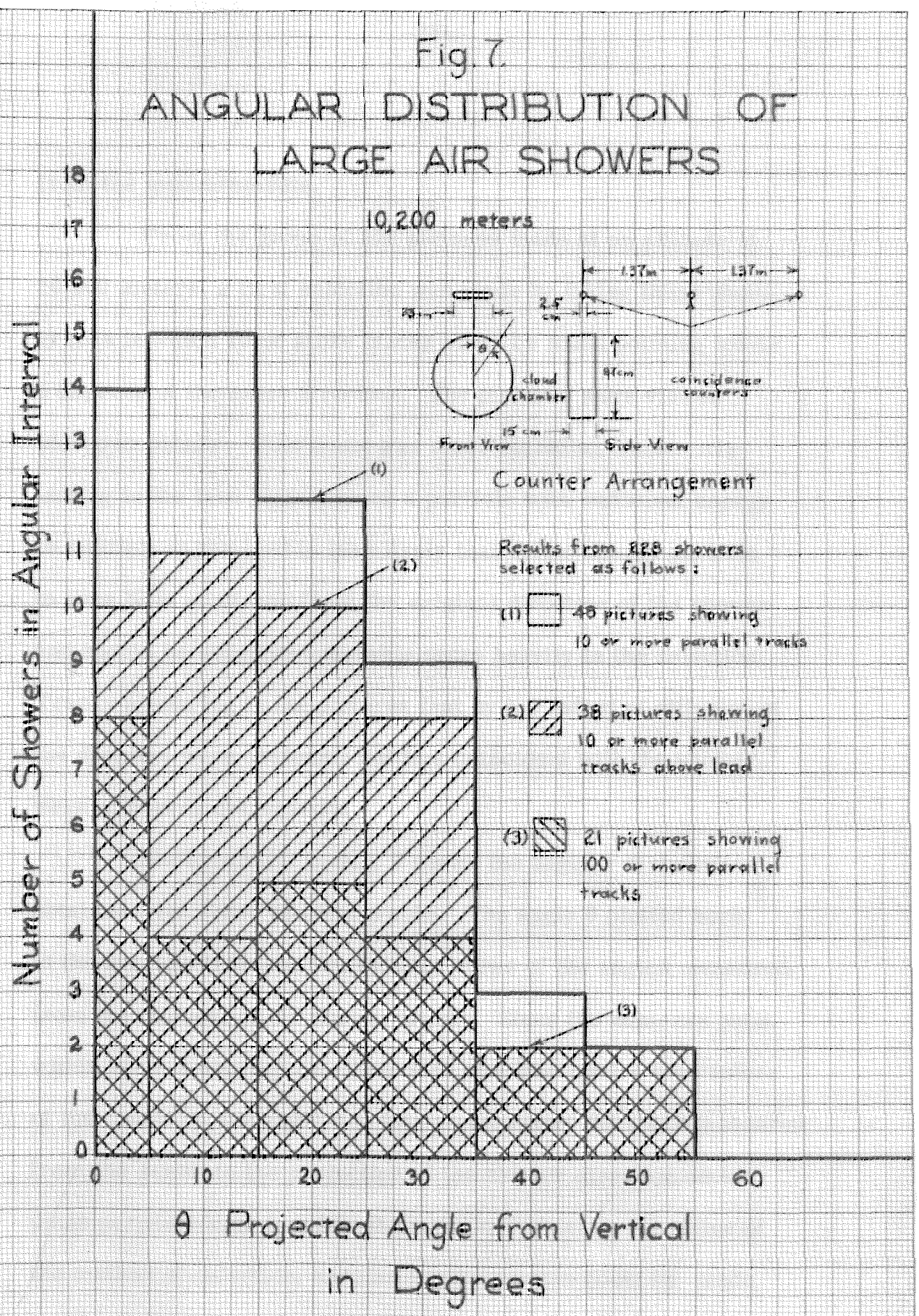

from the measurements.

From the group of 228 pictures made at an altitude of 10,200 meters, a first selection was made by taking those photographs in which 10 or more tracks could be found pointing within 5 degrees of the same direction. The pictures were viewed stereoscopically. This count was made including tracks originating in the lead plates, since a particle with sufficient energy to multiply in the lead is less likely than a low-energy particle to have been scattered from the original direction of the shower and should be weighted somewhat more heavily in the selection. Tracks appearing in the pictures that by the extent of diffusion of the droplets were obviously not time coincident with the shower, were of course disregarded.

Histogram (1) in Fig. 7 shows the angular distribution obtained from these 48 photographs. The angle θ plotted here is the average from the two camera views of the angles measured from the vertical of the shower tracks. Since the cameras point within about 5 degrees on either side of a line joining the centers of the counters, the angle θ is fairly accurately the angle measured from the zenith to the projection of the shower direction on a plane perpendicular to a line through the counters. By virtue of the method of selection, angular measurements could be made

within 5 degrees and in most photographs more precisely. Since this is considerably less than the angular interval used in the histogram, which is as small as is justifiable by the number of showers recorded, any error introduced in the actual measurement of the angles is of no great importance.

A theoretical calculation of the angular distribution of large showers has been made by M. M. Mills [1] on the basis of the present cascade theory of shower formation, from which the number and approximate distribution of shower particles produced by a particle of given energy at a given place in the atmosphere may be predicted.[2] If the primary particles responsible for the showers are assumed to be isotropically incident on the top of the atmosphere and of integral energy spectrum of the form $(\text{Energy})^{-1.8}$, the frequency per unit solid angle with which showers should trip the counter arrangement can be evaluated as a function of direction, which enters by way of determining the number of radiation units of atmosphere a shower must penetrate to reach a given elevation above the earth. Such assumptions have been justified by N. Hilberry [3] and H. Euler [4], for instance.

This frequency must in turn be modified to obtain the frequency of occurrence of projected angles, which is what was measured in the experiment. The complicated multiple integrals

involved have been set up and evaluated numerically by Mills for the particular experimental arrangement described above. The results were roughly checked by similar calculations based on the experimental measurement of the variation of shower frequency with altitude made by H. Kraybill[5] using, among other counters similarly arranged, the same set of counters from which he supplied the trigger pulse used to trip the large chamber.

A comparison of the calculated and experimental results is made in Fig. 8. Although the disagreement of the experimental point for any one angular interval may be explained with reasonable probability on the basis of statistical fluctuations resulting from the small number of observations, the overall appearance of the curves is in fairly marked disagreement. Half of the 48 shower ~~shower~~ angles measured fall within 17 degrees of the vertical, whereas the corresponding angle for the calculated curve is approximately 26 degrees.

A considerable difference between the two curves is not surprising, since the selection of showers for the experimental curve was made much more restrictive than for the calculated curve by adding to the requirement of the three-counter coincidence the requirement that 10 or more nearly parallel tracks be found in the photograph. This elimination of approximately

CALCULATED AND OBSERVED ANGULAR DISTRIBUTION OF LARGE AIR SHOWERS

Fig. 8

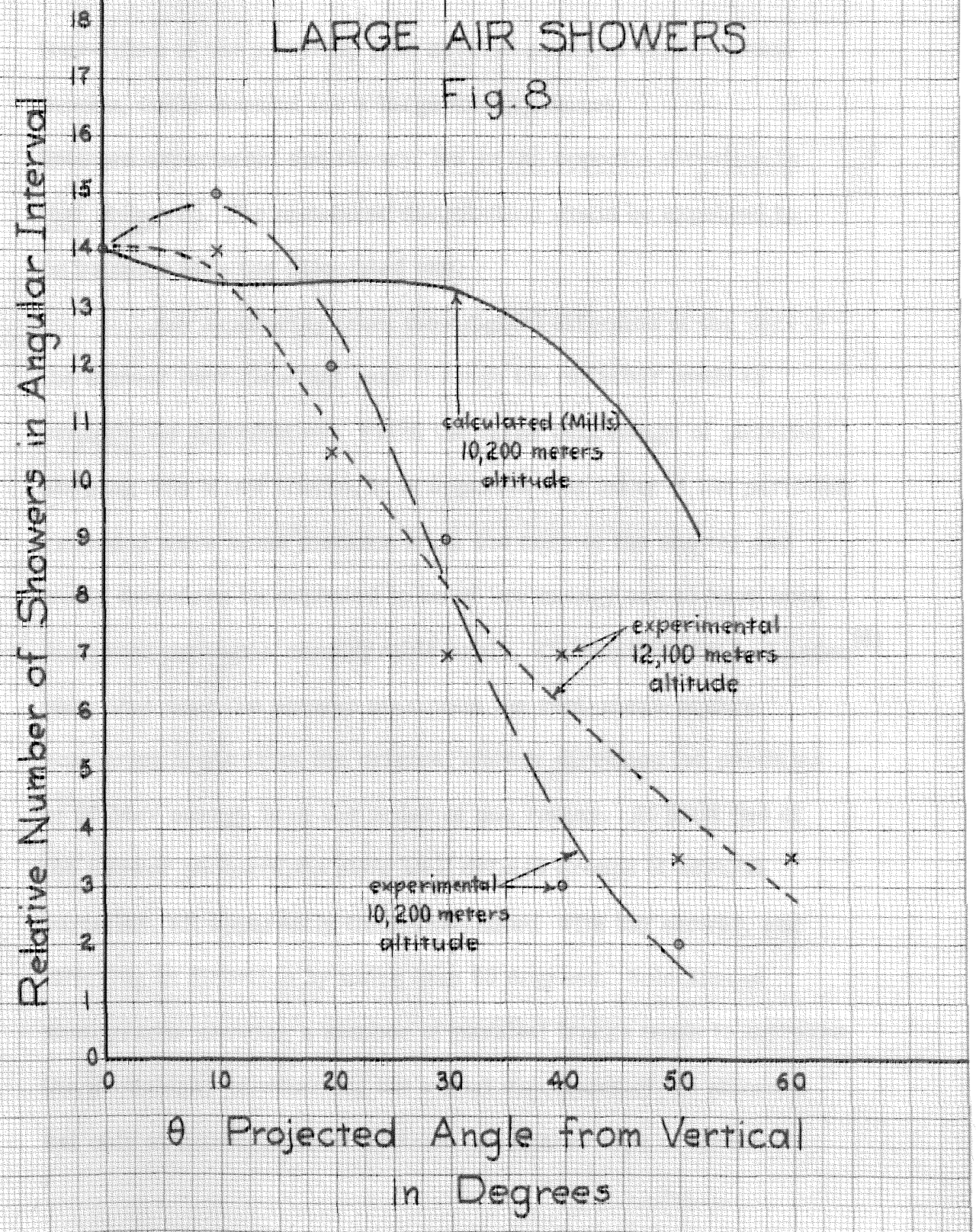

four-fifths of the pictures, plus several possible experimental errors, could account for a large disagreement between experiment and theory, but in the opposite direction to that observed. The measured distribution would be expected to be broader than the calculated one.

Any scattering from the original direction of the core of the shower particles that pass through the chamber tends to broaden the distribution. From the large percentage of pictures showing only a few tracks, it is apparent that many of the particles recorded were some distance from the core of the shower and would therefore be expected to be of low energy and to have been scattered through a considerable angle. Calculations by L. Landau[6] show that near the shower maximum the root-mean-square scattering angle from the original shower direction for particles of 30 Mev energy is of the order of one radian. At least two of the shower photographs show well defined groups of several particles, all apparently time-associated with the shower, and differing in direction by more than 45 degrees. Selection of photographs showing a number of parallel tracks tends to increase the probability of obtaining the actual directions of the showers but only at the expense of introducing another type of error.

In addition to favoring showers with nearby cores, this method of selection favors denser showers and therefore the directions from which denser showers come most often. At an altitude of 10,200 meters, the average shower-producing particle that arrives from a vertical direction has not traversed sufficient atmosphere to have multiplied to the maximum size at which the increasing absorption of particles, as the energy becomes more and more subdivided, again reduces the size. Hence a direction somewhat away from the vertical is favored by selecting denser showers, and this is confirmed, within the limitation imposed by the small number of observations, by histogram (3) in Fig. 7. This shows the angular distribution of 21 shower pictures selected as showing 100 or more nearly parallel tracks. Since tracks produced with counter-tripped operation of the chamber are somewhat diffuse, estimates of number of tracks are necessarily very rough. Although showers from very low angles as well as from the vertical are discriminated against in selecting showers of higher density, any attempt to correct for this selection in the region from perhaps 20 to 45 degrees, where the disagreement between the calculated and observed numbers is already very pronounced, only accentuates the disagreement.

Since tracks that had been produced by multiplication in the lead were counted in the 10-track selection process, the change in projected area of the lead plates with direction might be expected to favor showers from the vertical. However, this is at least in part offset by the change in apparent thickness with direction and the fact that elimination of low-angle showers from the front or back of the chamber broadens the projected-angle distribution. Iny any event, since this effect varies with direction no more rapidly than the cosine of the angle, no very marked broadening of the narrow experimental curve can be obtained from this source. A separate histogram (2) has been plotted in Fig. 7 that includes only those showers that showed 10 or more parallel tracks above the lead plates, and although this slightly broadens the distribution, the improvement is not very significant.

Showers that pass through the chamber from the side produce longer tracks in the rather flat cylindrical chamber and are therefore more noticeable than showers from the front or back with the same zenith angle. Any correction for this effect narrows the observed projected-angle distribution and again makes the disagreement more pronounced, as would any errors

introduced by the airplane not being exactly level at all times.

The only conclusion to be reached on the basis of the above arguments is that there is not satisfactory agreement between the observed angular distribution of large air showers and the distribution calculated from the present cascade shower theory.

Of the 44 pictures taken at an altitude of 12,100 meters, an angular distribution from 21 selected as having 3 or more nearly parallel tracks is plotted in Fig. 8. As might be expected, the distribution is somewhat broader than at 10,200 meters, since at both elevations showers from the vertical have not traveled through sufficient air to have multiplied to maximum size. Although the showers included in the distribution are too few to be in themselves significant, they add confirmation to the disagreement discussed above.

Some photographs typical of those showing a large number of shower tracks are presented in Fig. 9. The type of shower pictured in (a) and (b) of this figure is typical of what might be expected fairly close to the main core of a large air shower on the basis of the present shower theory. A fairly large number of parallel tracks, apparently having originated at a point in the

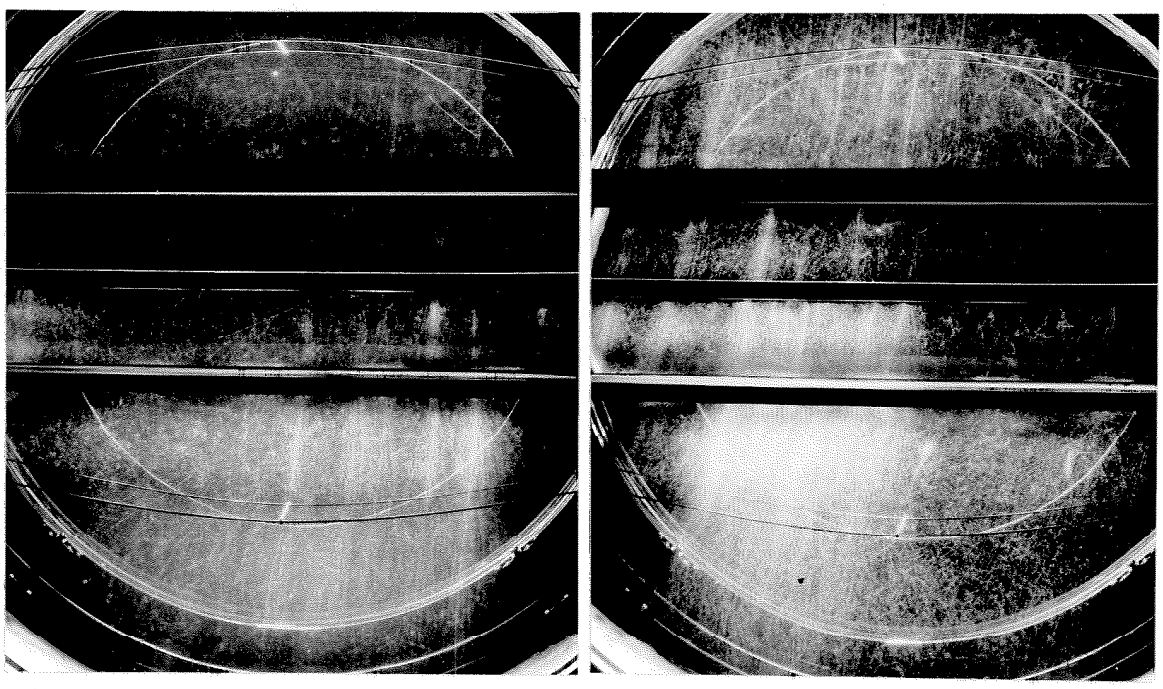

(a) (b)

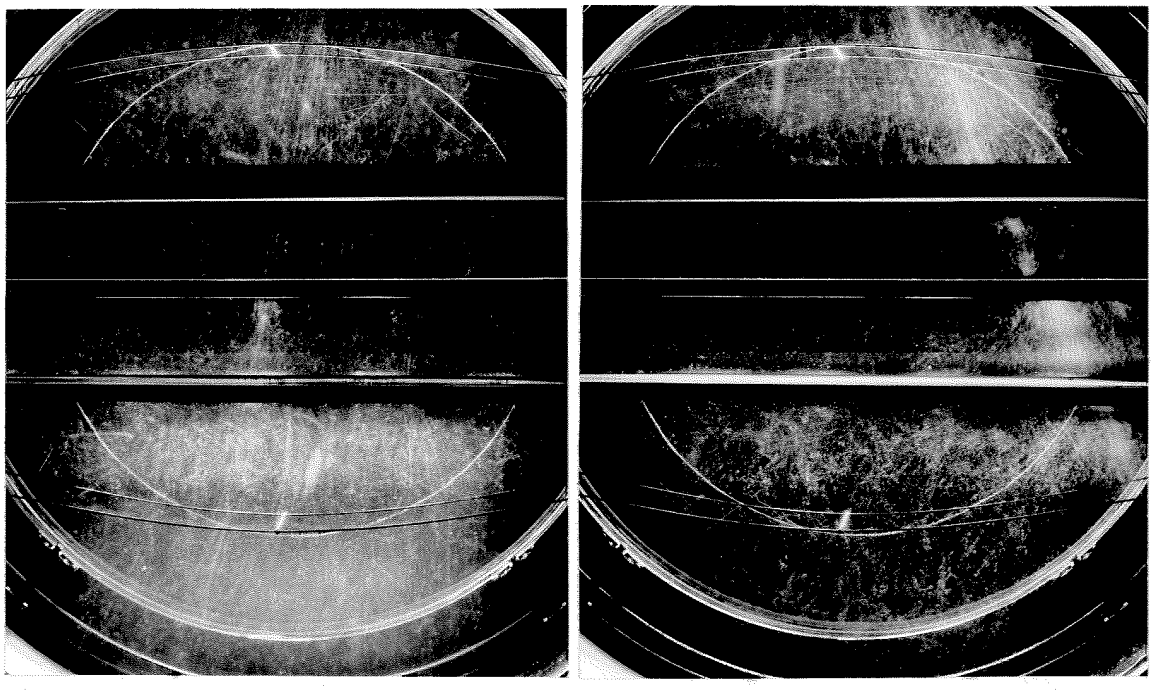

(c) (d)

Fig. 9. Photographs of large air showers.

atmosphere high above, multiply rapidly in the lead without too much angular spreading, indicating that the tracks are produced by electrons of high energy. A second type of photograph, shown in part (c) of Fig. 9, shows a part of the shower considerably farther from the main core. A number of tracks in the top of the chamber appear to radiate fanlike from a point only a short distance above the chamber, possibly in the hull of the airplane. Only a few of these tracks near the center of the fan were made by particles having sufficient energy to multiply into a small core under the lead; and although other shower tracks are visible than those in the fan, they also show relatively little multiplication. This seems a reasonable picture to expect at some distance out from the core, where only particles of lower energy that have been scattered through a considerable angle are found.

The photograph in part (d) of Fig. 9 is more difficult to understand. Here a single core of considerable size and very high density, even above the lead, strikes the lead and passes through with little spreading by scattering. No other cores of any size are visible in the chamber. If this is to be interpreted as a statistical fluctuation of the spatial distribution pictured in (a) and (b), it is a large fluctuation. Since at the present time no theoretical calculations have been published on the statistical

fluctuations to be expected in spatial distribution, no comparison with theory is possible. Of course, it is not necessarily true that all of the photographs are of different parts of the same type of shower rather than of entirely different types of showers. If some or all of the showers have a penetrating particle component, which has not been definitely established at the present time, the theory will require revisement, and possibly some of the features of the above experiments will then be explained.

No evidence for such a penetrating component could be found on the shower photographs. However, since identification of a mesotron requires that a separate track must be traced through the lead and observed not to multiply, such particles could be expected to be identified only when traveling singly. No conclusion can be drawn from the photographs as to the existence of particles in addition to electrons that may be traveling with the cores made up of dense bundles of tracks.

3.2. Evidence for Low-Mass Mesotron. The photographs in Fig. 10 show what is apparently an elastic collision between a particle of mass about 13 times that of an electron and an electron in the gas of the chamber. An explanatory diagram is given in Fig. 11. A second knock-on electron of shorter range also occurs along the same track, but this will not be discussed until a later paragraph. From the range of the electron, which stops in the gas, its velocity immediately after the impact is found to have been about 1/3 of the velocity of light, and comparison of the ionizations along the two tracks near the junction shows the heavier particle to have had about the same velocity. The masses of the two particles are therefore only about 5 per cent greater than their rest masses, and no relativistic corrections are needed for the accuracy desired. Since the energy transferred to the electron is about 50,000 eV while the binding energy of even the K-shell electrons of argon, the

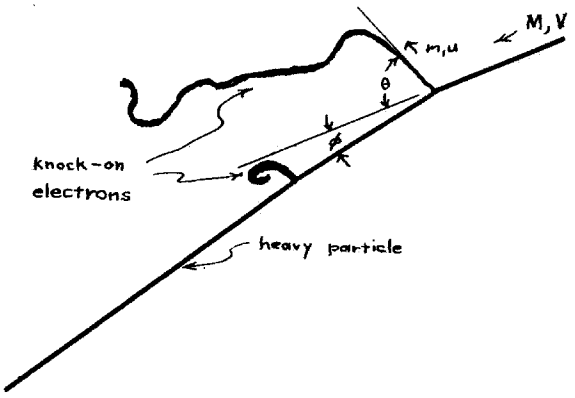

Fig. 11. Explanatory diagram for elastic collision shown in Fig. 10.

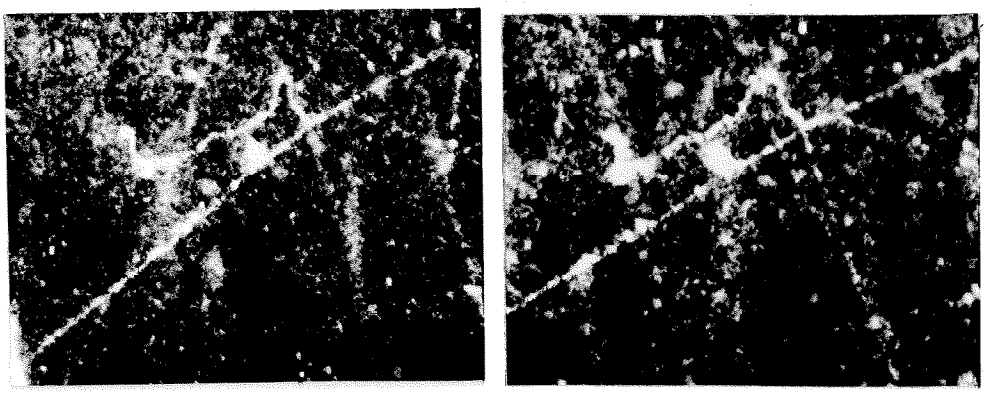

Fig. 10. Evidence for low-mass mesotron.

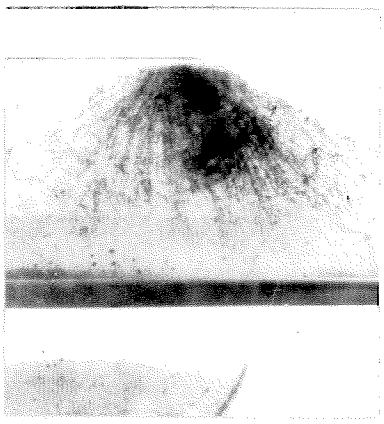

Fig. 12. (a)
Unusual shower.

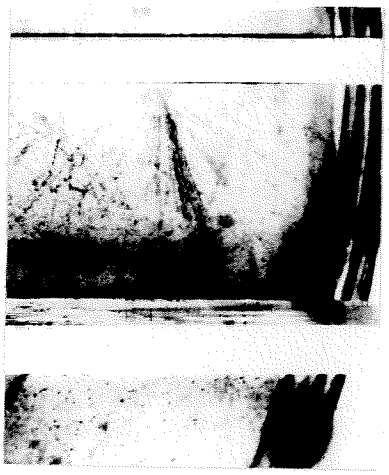

Fig. 12. (b)
Typical cascade shower.

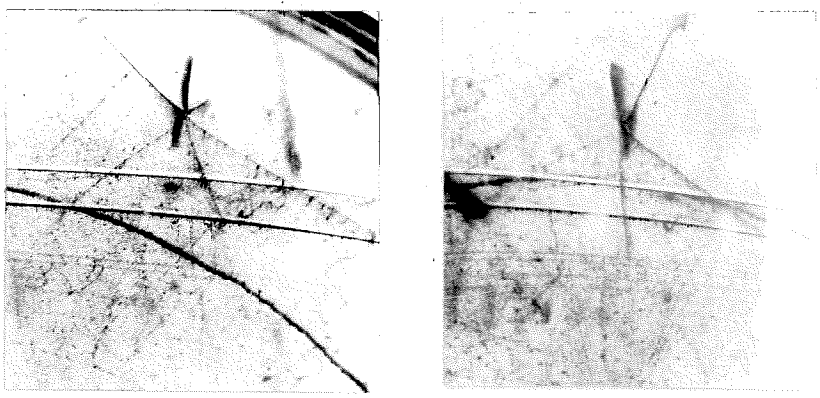

Fig. 13. Nuclear disintegration originating in gas of chamber.

heaviest atom in the chamber gas, is only 3,200 eV, the collision may be considered elastic and the laws of conservation of momentum applied. The following relations are obtained.

$$M/m = \frac{\sin (2\theta + \phi)}{\sin \phi} \qquad (1)$$

$$u/v = (M/m)(\sin \phi / \sin \theta) \qquad (2)$$

$$u = 2V\frac{M}{M + m} \cos \theta \qquad (3)$$

Here m and u are the mass and velocity of the electron and M and V the mass and velocity of the heavy particle before the collision. Since the heavy particle loses only a small fraction of its energy, its velocity v after the collision is approximately equal to V.

The position in space of the track in the chamber was such that there were large components along the directions toward the two cameras. Consequently the deflections of the heavy particle are considerably accentuated. To measure the actual angles in space, the two stereoscopic views were projected on a screen which was then tilted until the two projections coincided, thus giving the plane of the collision in space. The values of θ and ϕ obtained, when substituted in equation (1) give the result

that the mass of the heavy particle is approximately 13 times that of the electron.

Most of the error in the mass ratio probably results from uncertainty in the measurement of θ because of scattering in the electron track. The measured value of 60 degrees for θ gives a value for the mass ratio only slightly smaller than the maximum ratio that can be obtained for any value of θ so that the actual mass must be lower as far as any error here is concerned. If the value of θ had been in error by much more than the amount needed to halve the mass ratio given, the relative ionizations of the two tracks would be noticeably inconsistent with the relative velocities required to satisfy equation (3). An error in the measured value of 3.8 degrees for ϕ raises or lowers the calculated mass in inverse proportion to the error.

Consider now what other possible interpretations might be given to the track in Fig. 10. The possibility that the track could have been produced by an electron can be immediately eliminated on the basis of the ionization and degree of multiple scattering of the track. Although the use of high-contrast printing paper has lost a good deal of resolution and made the track appear somewhat lumpy on the print, examination of the original

negative leaves little doubt that the ionization of the track is 5 or 10 times the minimum value and about equal to that of the knock-on electron at the point of the junction, indicating that the two particles had about the same velocity. If both tracks are those of electrons, they would then be expected to show about the same scattering, which is not the case.

The remaining possibility that the track was made by a mesotron of 200 electron masses or a still heavier particle will now be considered. Even if the angle θ is completely falsified by a single-scattering of the electron by a nucleus immediately after the knock-on collision, the maximum possible mass ratio obtainable for any angle θ is approximately $\cot \phi$, which is only slightly larger than the calculated value. This leaves only the possibility that the track was caused by a mesotron or proton that was scattered by a nuclear collision very close to the point where the knock-on collision occurred. The probability of finding such a chance track similar to that shown in Fig. 10, with ionization and scattering that are at all consistent with a mass below that of the usual mass-200 mesotron, may be roughly evaluated as follows.

Since velocities very much less or greater than that of the particle being considered either rule out entirely a particle of intermediate mass or allow no conclusion whatsoever to be drawn,

the evaluation of the probability, which is only intended to give the order of magnitude, will be made for this velocity of 1/3 the velocity of light. Also, since a proton is less likely to be deflected than a mesotron of the same velocity, while having the same probability of producing a knock-on electron of given energy, only a mass-200 mesotron will be considered. Only a small fraction of the kinetic energy of the mesotron is lost in such a collision so that spin forces may be neglected and the probabilities of the occurrence of knock-on electrons and nuclear deflections from the electric forces evaluated by the classical formulas. The Rutherford formula[7] for the probability of a single deflection of greater than the angle ϕ of a particle of mass M and velocity V in traversing a distance t of material having N atoms of atomic number Z per unit volume is as follows, where e is the electronic charge.

$$P(\phi) = \frac{\pi N t Z^2 e^4}{M^2 V^4} \cot^2 \phi \qquad (4)$$

Using for t the average length of a track in the large chamber, which is about 30 cm, and for ϕ a value of one degree, since a smaller deflection than this could scarcely be determined as a single scattering, the probability for finding a mesotron

track in the chamber with a noticeable single scattering is about $\frac{1}{2}$.

Similarly, the Rutherford formula[7] for the probability of a particle producing a knock-on electron of energy greater than E, using the symbols defined above and m for the electronic mass, is as follows.

$$P(E) = \frac{2 \pi e^4 N Z t}{m V^2 E} \qquad (5)$$

Since in the track in Fig. 10 the knock-on collision may be ascertained to occur within less than 0.1 cm of the point of deflection of the track, a value of t equal to 0.2 cm substituted in the formula gives the probability that a knock-on will occur within 0.1 cm of a chance deflection. A value of E of 5,000 eV will be used, since any lower energy is inconsistent with the momentum required for a deflection of as much as one degree for the type of track being considered. The resulting probability is about 0.04.

Furthermore, in an elastic collision the tracks must be coplanar. By view the track of Fig. 10 stereoscopically, it may be seen that the plane of the knock-on track at the junction is no greater than 10 degrees from the plane formed by the deflected

track. The probability of this occurring by chance is about 0.05.

However, two such knock-on collisions satisfying the general requirements discussed above have occurred on the same track in Fig. 10. Therefore the above probabilities must be combined by mulitplication and then squared. In addition the ratio of the ranges of the two knock-on electrons checks with the measured deflections within about 15 per cent. The probability of this occurring by chance has been estimated by rough numerical integration of differential probabilities obtained from equation (5) to be less than 0.1.

The resultant probability that a chance mesotron track occur that would fit the interpretation of a low-mass mesotron in the manner of the track in Fig. 10 is about one in ten million. Although several thousand tracks of the general type being considered in the probability calculation were examined in finding the track shown in Fig. 10, the odds are still against this being an accidental coincidence.

In addition to the two tracks mentioned, several more have been found that show a probability that, while not nearly as small as that calculated above, is reasonably in favor of the interpretation of a knock-on electron from a low-mass mesotron. If

the above arguments are considered as convincing as to the existence of such a particle, these tracks furnish additional data for making a mass determination.

Another type of evidence for a low-mass mesotron has been found in the multiple scattering and ionization of several tracks. Although estimates of multiple scattering and ionization are severely limited in accuracy by the restrictions discussed in section 2.3, at least two tracks have been found that, even with the greatest reasonable allowance for errors, can not be interpreted as having a mass as small as that of an electron or as large as 200 times the mass of an electron.

In all of the above reasoning the particle has been assumed to have one electronic unit of charge.

3.3. Special Events. In examining the 3500-odd photographs, a large number of unusual and anomalous tracks were found. Since some 1500 such occurrences were listed, it is impossible to mention more than a few in this thesis.

An interesting type of shower originating in one of the lead plates is shown in Fig. 12 (a). At least two similar showers, in which very large numbers of electrons emanate from a comparatively thin lead plate, have been photographed by other obser-

vers, one by Shutt[8] and one by Street[9]. The first such shower, which was obtained by Street in 1939, was originally explained as an unusually large statistical fluctuation in the cascade shower theory. The probability of such an occurrence can be approximated from a formula developed by Furry[10] for the probability of obtaining n particles by cascade multiplication of a high-energy electron in a thin plate of heavy material if the average number obtained is n_0.

$$(P(n)) = \frac{(1 - 1/n_0)^{n-1}}{n_0} \qquad (6)$$

For the shower in Fig. 12, $n_0 = e^3 = 20$. A conservative estimate for n is 100. The calculated probability then is about 0.0003.

Although even this rather low probability is not out of reason considering the large number of photographs taken, another feature that the three showers of this type have in common makes the fluctuation hypothesis still more unlikely. All three showers show tracks spread more or less uniformly through a wide angle without the core of high-energy particles retaining the direction of the original particle that is typical of cascade showers.

Compare, for instance, the shower shown in Fig. 12 (b), which is typical of the showers produced by a single electron entering the lead plates. In confirmation of this idea, of the 40 particles of the 80-particle shower in Shutt's photograph that struck a 1-cm lead plate, none penetrated to emerge on the other side. Although most of the particles in the shower shown in Fig. 12 (a) miss the $1\frac{1}{2}$-cm lead plate, here, likewise, none of the particles striking the plate emerge on the other side.

In view of the exceedingly low probability of producing such a large number of uniformly low-energy electrons by the cascade process, this does not seem to be a suitable explanation for the three observed showers of this type. Additional interesting properties common to the three showers are that no tracks of ionizing particles that might be responsible for the shower appear above the lead plate in wich the shower originates, and no heavily ionizing tracks are visible.

Some of the more interesting special events observed in the chamber have been in the form of disintegrations occurring in the gas of the chamber, where all of the ionizing particles participating in the event leave visible tracks. Although many of these are the familiar nuclear disintegrations, such as the one shown

in Fig. 13, some exhibit unusual properties, and a more detailed analysis of these photographs may be worthwhile. With this in mind a list of 58 photographs showing disintegrations occurring in the gas has been prepared for the use of anyone who may in the future be interested in this subject.

References

1. Mills, M. M., A Study of the Altitude Dependence of the Large Cosmic-Ray Showers, Ph.D. Thesis, California Institute of Technology, 1948.

2. Heisenberg, W., Cosmic Radiation, 18-40, Dover Publications, New York, 1946.

3. Euler, H., Z. f. Physik (1940, 116, 73.

4. Hilberry, Norman, Physical Review (1941), 60, 1.

5. Kraybill, H. L., Physical Review (1948), 73, 632.

6. Landau, L., Journal of Physics of U.S.S.R. (1940), 3, 237.

7. Rutherford, E., Chadwick, J., and Ellis, C. D., Radiations from Radioactive Substances, 194 and 441, Cambridge Press, 1930.

8. Shutt, R. P., Physical Review (1946), 69, 261.

9. Street, J. C., Journal of the Franklin Institute (1939), 227, 569.

10. Furry, W. H., Physical Review (1937), 52, 569.